Fractal features of a crumpling network in randomly folded thin matter and mechanics of sheet crushing

Alexander S. Balankin,[1] Antonio Horta Rangel,[2] Gregorio García Pérez,[1] Felipe Gayosso Martinez,[1] Hugo Sanchez Chavez,[1] and Claudia L. Martínez-González[1]

[1]*Grupo "Mecánica Fractal," ESIME-Zacatenco, Instituto Politécnico Nacional, México D.F., Mexico 07738*

[2]*Universidad de Guanajuato, Guanajuato, Mexico 36250*

(Received 25 January 2013; revised manuscript received 24 April 2013; published 20 May 2013)

We study the static and dynamic properties of networks of crumpled creases formed in hand crushed sheets of paper. The fractal dimensionalities of crumpling networks in the unfolded (flat) and folded configurations are determined. Some other noteworthy features of crumpling networks are established. The physical implications of these findings are discussed. Specifically, we state that self-avoiding interactions introduce a characteristic length scale of sheet crumpling. A framework to model the crumpling phenomena is suggested. Mechanics of sheet crushing under external confinement is developed. The effect of compaction geometry on the crushing mechanics is revealed.

DOI: 10.1103/PhysRevE.87.052806 PACS number(s): 89.75.Fb, 61.43.Hv, 05.45.Df, 46.65.+g

I. INTRODUCTION

Randomly folded configurations of thin matter are ubiquitous in nature and engineering. Examples range from crumpled nanosheets of graphene [1–3], graphene oxide [4–6], and proteins [7–9], to hand folded paper [10–15] and geological formations [16]. Even when the crumpling processes appear quite haphazard, the geometry of randomly folded materials are well defined in a statistical sense and rather well reproducible in experiments [1–15], because the topology and self-avoiding interactions are the two most important factors when dealing with the crushing of thin matter [17–19]. Accordingly, the studies of crumpling phenomena remain an active area of research, both theoretically and experimentally (see, for example Refs. [20–43] and references therein).

A remarkable feature of thin matter is that its stretching rigidity is much more than the bending rigidity. Consequently, the curvature imposed on an elastic sheet by external confinement is concentrated largely in sharp creases and developable cones [44], whereas a major fraction of sheet area remains relatively flat and unstrained [45]. In the limit of an infinitely thin sheet, creases and developable cones asymptote to lines (ridges) and points (vertices) in accordance with the Gauss's *theorema egregium* which states that surfaces could not change their Gaussian curvature without changing distances and so sheet elements that are curved in two directions must be strained [18]. Sharp ridges which meet at pointlike vertices form the branched crumpling network with an anomalously larger resistance to hydrostatic compression [2,6,19,23,27–29,46,47], but a very low stiffness under axial compression [13,15,31,43]. In this context, it was shown that the total energy stored in a single ridge scales with its size l as $E_r \propto h^3(l/h)^{1/3}$, where h is the sheet thickness [44]. Furthermore, it was assumed that that when a square sheet of size L is folded in a ball of diameter R, the mean ridge length and the total number of ridges obey simple scaling relations $\langle l\rangle \propto R$ and $N_r \propto (L/\langle l\rangle)^2 \propto R^{-2}$. Accordingly, the total energy stored in the crumpling network formed in the sheet folded in a ball is suggested to scale as $E_N \propto N_r E_r(\langle l\rangle) \propto h^{8/3}L^{1/3}K^{5/3}$, where $K = L/R$ is the compaction ratio [44]. If so, the folding force $F = \partial E_N/\partial R$ should scale with the ball diameter as $F \propto L^2(h/R)^{8/3}$. Consequently, a set of balls folded from elastic sheets of different sizes $L \gg h = \text{const}$ under the same force $F_0 = \text{const}$ is expected to obey the fractal mass scaling relation,

$$R^D \propto L^2, \tag{1}$$

with the fractal dimension $D = 8/3$. Numerical simulations of phantom elastic sheets crushing under hydrostatic compression [23] have confirmed the scaling relation (1) with $D = 8/3$. However, in the case of self-avoiding elastic sheets, the fractal dimension defined by Eq. (1) is less than $8/3$ due to the effect of self-avoiding interactions [23]. Accordingly, based on scaling arguments, it was argued [33] that in the case of self-avoiding sheet crushing the mean ridge length and the total number of ridges both should scale with L and K as

$$\langle l\rangle \propto LK^{-\alpha} \quad \text{and} \quad N_r \propto (L/\langle l\rangle)^2 \propto K^{2\alpha}, \tag{2}$$

respectively. Accordingly, the total elastic energy stored in the ridges is suggested to scale as

$$E_N \propto N_r\,(\langle l\rangle/h)^{\beta} \propto (L/h)^{\beta}K^{\alpha(2-\beta)}, \tag{3}$$

where the scaling exponents are α and β; $\alpha \geqslant 1$ and $1/3 \leqslant \beta < 2$ [33]. Consequently, it is expected that the diameter of a ball folded from the crumpled sheet depends on the hydrostatic confinement force F as

$$F \propto L^{2\mu/D}R^{-\mu}, \tag{4}$$

where

$$\mu = 1 + (2-\beta)\alpha, \tag{5}$$

and so, a set of balls folded from self-avoiding elastic sheets of different sizes under the same confinement force will obey the fractal relation (1) with the mass fractal dimension

$$D = 2 + \frac{2(1-\beta)}{\beta + (2-\beta)\alpha}. \tag{6}$$

In numerical simulations of elastic self-avoiding sheets [33] it was found that relations (1)–(4) hold in the range of $2.5 \leqslant K \leqslant 8$ with $\mu = 3.83 \pm 0.11$, while $\alpha = 1.65$, $\beta = 1/3$, and $D = 2.5 \pm 0.1$. Furthermore, it was argued [33] that

these values within error bars are numerically consistent with relationships (5) and (6); nonetheless quite different values $D = 2.3 \pm 0.1$ and $\mu \approx 4$ were found in the numerical simulations reported in Ref. [23]. Moreover, the results of numerical simulations in Ref. [33] suggest that the plastic deformations in crumpling ridges lead to decrease of D, whereas α, β, and μ remain unchanged within the error of estimations. So, it was assumed that scaling relationships (5) and (6) are not valid for elastoplastic materials (see Ref. [33]). However, in contrast to this, in experiments with predominantly plastic sheets it was found that plastic deformations lead to increase of μ and decrease of D [29] in qualitative accordance with Eqs. (5) and (6). On the other hand, in the case of elastoplastic sheets, such as paper, it was observed that once the folding force is withdrawn, the ball diameter logarithmically increases in time due to elastic strain relaxation [11–15]. In this way, it was found that after complete relaxation during approximately 10 days the final ball diameter is almost independent of the force applied during the sheet crushing [11]. Consequently, a set of paper balls after compete elastic strain relaxation is characterized by the material dependent fractal dimension D [11,12]. It is also pertinent to note that in experiments with randomly folded sheets of different materials it was found that D varies in the range of $2.1 \leqslant D \leqslant 2.7$ (see Refs. [3,5,6,10–14,19,25,27,29,30,35]).

In this context, it should be emphasized that the fractal dimension D is a measure for how the sheet size affects its compactification (see Refs. [3,6,12,19,29]), but tell us nothing about the internal structure of a folded ball [48]. Furthermore, it is a straightforward matter to understand that the scaling exponent μ depends on the crumpling geometry (hydrostatic, radial, or axial confinement) [43]. Therefore it was proposed to relate μ to the fractal dimension of compaction geometry D_c (see Ref. [43]). Specifically, the crumpling of a sheet confined in the cylinder by the axial force is characterized by $1 < \mu = D_c < 2$, whereas the sheet crushing under the hydrostatic compression is characterized by $4 < \mu < 6$ [43].

Dimension numbers D and D_c characterize different aspects of crumpling phenomena. Namely, D_c governs the scaling relation (4) between the applied force and the compaction of the crumpled sheet [43], whereas D characterizes the scaling relation (1) for the set of sheets of different sizes crushed by the same force. Nonetheless, it is easy to understand that D should depend on the crumpling geometry and so on D_c. Moreover, although the radial mass distribution in a randomly folded sheet is rather isotropic (see Refs. [30,38]), it was found that the internal arrangements of randomly folded sheets also exhibit statistical scaling invariance [12,14,30] characterized by the scaling behavior of the spatially averaged mass density $\langle \rho(r) \rangle_R \propto \rho_0 r^{D_l - 3}$, where ρ_0 is the sheet mass density and $\langle \cdots \rangle_R$ denotes the average overall possible position of cube (sphere) of size $r \ll R$ within the folded ball of diameter R, while D_l is the local mass dimension and $\langle \rho(R) \rangle_R = 6\rho_0 L^2 h / \pi R^3$. Hence, the folded structure can be viewed as a fractal porous medium with an almost homogeneous distribution of pore space (such as, for example, percolation backbone [49] and soils [50,51]), rather than as a fractal growing from the mass center (such as clusters formed by the diffusion limited aggregation [52]). In the x-ray tomography experiments with randomly folded aluminum foils it was found that the local fractal dimension of folding arrangements is an increasing function of compaction ratio, such that $2.2 \leqslant D_l (2 < K \leqslant 6.25) \leqslant 2.8$ [30]. In contrast to this, the folding configurations of randomly crushed papers after elastic strain relaxation are characterized by the universal local fractal dimension $D_l = 2.64 \pm 0.05 \approx 8/3$ [12,14], whereas D is material dependent. Therefore, the local density in a hand folded paper ball after elastic strain relaxation obeys the following scaling behavior:

$$\langle \rho(r) \rangle_R \propto r^{D_l - 3} R^{D - D_l}, \tag{7}$$

where $D \leqslant D_l$ [12,14]. Furthermore, it is reasonable to expect that the local fractal dimension of folding arrangement (D_l) is dependent on the crumpling geometry (characterized by D_c), as well on the rheological properties of the sheet. That is, ideally elastic, such as rubber [31]; elastoplastic, e.g., paper [12]; and predominantly plastic, e.g., aluminum foil [30] are expected to obey Eq. (7) but with different D_l.

Another important issue is the geometry of the crumpling network. Understanding the three-dimensional arrangement of an interacting set of crumpling creases is a formidable challenge, and it is crucial to understanding of the geometric and mechanical properties of randomly folded matter [5,11,15,16,18,19,23,26,28,31–35,44,46,47]. To this respect, it is pertinent to note that the second relation in Eq. (2) is based on the assumption that the crumpling network is effectively two dimensional on the length scale $l \geqslant \langle l \rangle$. However, the data reported in Ref. [11,53] suggest that the crumpling networks formed in paper sheets display statistical scale invariance and within a bounded interval of length scale $\langle l \rangle \leqslant \Delta < R$ are characterized by the fractal dimension $D_N^{(2)} < 2$ [53]. If so, the total number of ridges scales with the sheet size as $N_r \propto (L/\langle l \rangle)^{D_N^{(2)}}$, rather than according to the second relation in Eq. (2). Furthermore, it is reasonable to guess that in sheets of finite rigidity and thickness the mean ridge length $\langle l \rangle$ depends on h, which is not accounted for by the first relation of Eq. (2). Besides, one can suppose that due to long-range correlations in the crumpling network the scaling exponent β in Eq. (3) can deviate from its value $\beta = 1/3$ derived for a single ridge.

To clarify these points, in this work we performed experimental studies of scaling properties of crumpling networks. Furthermore, to characterize the dynamics of the crumpling network, we determined its spectral dimension. Experiment details and results of experimental study of crumpling network impressions on the unfolded flat sheets are reported in Sec. II. Section III is devoted to analysis and discussion of experimental findings. Specifically, the universalities in the scaling properties of crumpling networks are discussed. The fractal dimensionalities of the crumpling network in the folded configuration are established on the basis of scaling arguments. The mechanics of sheet crushing is developed. The main results and conclusions are outlined in Sec. IV.

II. EXPERIMENTAL STUDIES

Paper crushing offers a convenient economical means to study crumpling phenomena. When a paper sheet is crushed by hand into a small three-dimensional ball, large deformations of paper lead to formation of irreversible scars leaving the

crumpling network impression on the sheet. This permits the study of crumpling networks on the unfolded sheets [11,26]. Accordingly, in this work, we study the static and dynamic properties of crumpling networks formed in hand crushed *Biblia* paper of thickness 0.039 ± 0.002 mm. Mechanical properties of this paper were reported in Ref. [11]. Besides, in Refs. [11,12], it was found that a set of balls folded by hand from square sheets of different sizes of this paper, after elastic strain relaxation, is characterized by the global fractal dimension $D = 2.30 \pm 0.05$, whereas the statistical distribution of ridge length in unfolded crumpling networks exhibits a crossover from the log-normal distribution at low K to the gamma distribution at larger confinement ratios [12,31]. At the same time, it was found that the local fractal dimension of folding configurations $D_l = 2.64 \pm 0.05$ is independent of the sheet size and confinement ratio [12,14].

A. Experiment details

In this work, the square sheets of edge size $L = 5$, 10, 15, and 20 cm were crushed by hand into approximately spherical balls of diameter R with four different initial confinement ratios $K = K/L$ repeated two times with sheets of each size (32 balls in total). After complete strain relaxation during 10 days (see Refs. [11,12]), 16 balls were cut in half to obtain photographic images of ball intersections with planes (see bottom inset in Fig. 1). The box-counting fractal dimensions $D_{\text{cross}}^{\text{plane}}$ of each of 32 digitized images (see top inset in Fig. 1) were determined by the box-counting method (see Fig. 1) with the help of the BENOIT1.3 software [54].

The rest of the 16 balls were unfolded and flattened to study the crumpling network impressions. Accordingly, after unfolding the ridges stamped on sheets were marked by pencil (see Ref. [11]) and the resulting images were digitized (see Fig. 2) to determine the coordinates and degrees of vertices. Furthermore, the fractal dimension of each crumpling network impression ($D_N^{(2)}$) was measured by the box-counting method using the BENOIT1.3 software [54], whereas the fractal dimension of shortest path between two randomly chosen vertices of the crumpling network impression was obtained

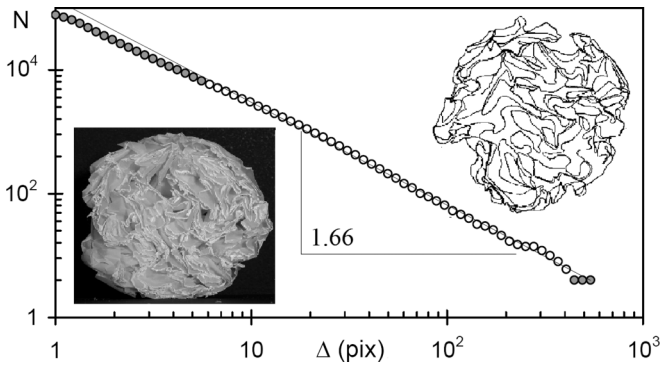

FIG. 1. Log-log plot of number of boxes covering the image of intersection (N) versus box size Δ (pixels); symbols: experimental data averaged over 32 images of 900×900 pixels; straight line: power-law fitting (full circles are excluded from fitting). Insets show typical photo and digitized image of intersection.

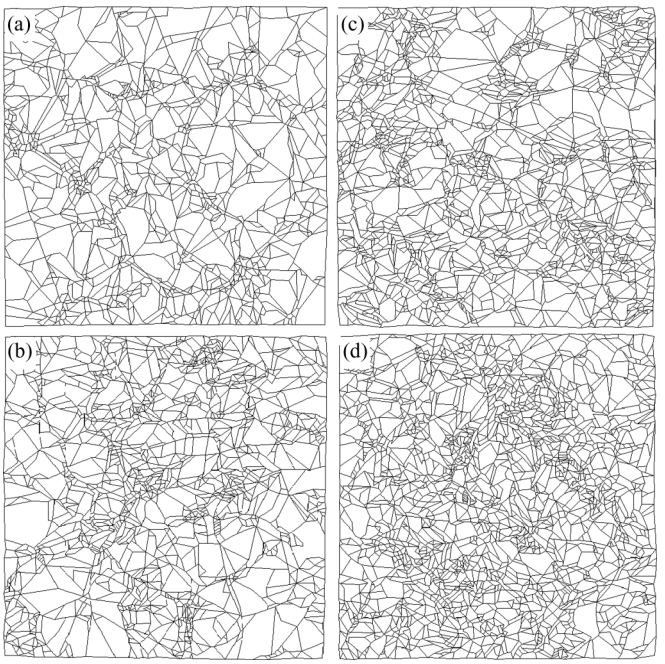

FIG. 2. Digitized images of crumpling networks stamped on unfolded sheets of edge size $L = 10$ cm from balls folded with the confinement ratios $K =$ (a) 3.33, (b) 4, (c) 4.76, and (d) 5.6, respectively.

from the scaling behavior,

$$\ell_{\min} \propto \ell_e^{d_{\min}^{(2)}}, \tag{8}$$

where $\ell_{\min}$ and ℓ_e are the chemical and Euclidean distances between the chosen vertices, respectively [55,56]. Consequently, the chemical dimension of crumpling network impression was calculated using the relationship $d_\ell^N = D_N^{(2)}/d_{\min}^{(2)}$ [55].

The chemical dimension quantifies how the "elementary" structural units (ridges) are "glued" together to form the entire fractal structure and so tells us "how many directions" the observer feels in the configuration space of the crumpling network by making *static* measurements. Hence d_ℓ^N determines the number of independent coordinates needed to define the position of a point vertex on the crumpling network. However, the number of dynamic degrees of freedom is equal to the spectral dimension d_s^N which governs the density of vibration modes with frequency ω as $\Omega(\omega) \propto \omega^{d_s - 1}$ and thus determines the scaling behavior of local energy distribution (Lagrangian) in the crumpling network (see Ref. [57]). In this work, the spectral dimension of each crumpling network was determined using the scaling behavior,

$$P_0 \propto n^{-d_s/2}, \tag{9}$$

of the probability $P_0(n)$ to find (still or again) the random walker (RW) at step n at the randomly chosen starting vertex [58]. As pointed out in Ref. [58] $P_0(n)$ exhibit a shorter transient regime than the probability of first return. This allows the determination of the spectral dimension with a smaller number of steps. We tested our program using the 6-iteration of the Sierpinski gasket to obtain $d_s = 1.34 \pm 0.06$ in simulations with 10^5 RW trajectories of 10^4 steps each, whereas the

exact value (in the limit of infinite number of iterations) is $d_s = 2\ln 3/\ln 5 = 1.3652\ldots$ [59].

Regarding the use of power-law fits, it is imperative to point out that ranges of variations of some parameters (L, K, $\ell_{\min}$, and box sizes in the measurements of box-counting dimensions) are rather small. In this context, it is pertinent to note that in experimental and numerical studies of randomly crumpled two-dimensional materials the ranges of L and K variations are always of the order or less than one decade due to their nature and technical limitations (see, for example, data fittings in Refs. [5,10–14,19,22–37,43]). To handle this limitation, in this work the χ^2 tests for goodness of fit were performed to verify the relevance of the power-law scaling in comparison with other fits in each case.

B. Experiment findings

Making use of the BENOIT1.3 software, we found that the ball intersections with plane (cuts) are characterized by the fractal $D^{\text{plane}}_{\text{cross}} = 1.66 \pm 0.06$ (see Fig. 1) which is independent of the sheet size (L) and the ball diameter after complete relaxation of elastic strains ($R_{\text{relax}} > L/K$). We noted that this value is consistent with the fractal dimension of ball intersections with straight strings $D^{\text{line}}_{\text{cross}} = 0.64 \pm 0.06 = D^{\text{plane}}_{\text{cross}} - 1$ [12], as well as with the statement of universality of the local fractal dimension after elastic strain relaxation [14]. Therefore, the intersection of a folded sheet with a two-dimensional plane can be roughly treated as the Cartesian product of the Cantor-set-like set of dimension $D^{\text{line}}_{\text{cross}}$ and a one-dimensional circle Figure 7.3 from Reference [60]). Hence, taking into account the isotropy of hand folded balls, the folding arrangement can be viewed as Cartesian products of the Cantor-set-like set with randomly deformed sphere, such that $D_l = D^{\text{line}}_{\text{cross}} + 2 = D^{\text{plane}}_{\text{cross}} + 1 \approx 8/3$. It should be emphasized that this universal value characterizes the scale invariance of randomly folded elastoplastic sheets such as paper only after the elastic strain relaxation when the self-avoiding interactions become negligible (see Refs. [12,14]).

In studies of crumpling networks we found that the numbers of vertices N_v and ridges N_r both scale with the sheet size and confinement ratio as

$$N_v \propto N_r \propto \left(\frac{L}{h}\right)^{\phi} K^{\gamma}, \tag{10}$$

where the scaling exponents

$$\phi = 0.6 \pm 0.1 \quad \text{and} \quad \gamma = 1.46 \pm 0.05 \tag{11}$$

are found to be independent of the sheet size and confinement ratio [see Fig. 3(a)], such that the node degree distribution remains invariant under the increase in the sheet size and/or compression ratio with the universal mean

$$\langle k \rangle = 2N_r/N_v = 3.5 \pm 0.1 \tag{12}$$

[see Fig. 3(b)] and an exponentially decaying tail consistent with the fitting by a log-normal distribution suggested in Ref. [26]. We also noted that the data reported in Table 2 of Ref. [26] are also consistent with the universal value (12). Although the ranges of L and K variations in Eq. (10) are rather small, the χ^2 test for goodness of fit confirms the relevance of the power-law scaling in comparison with other fits.

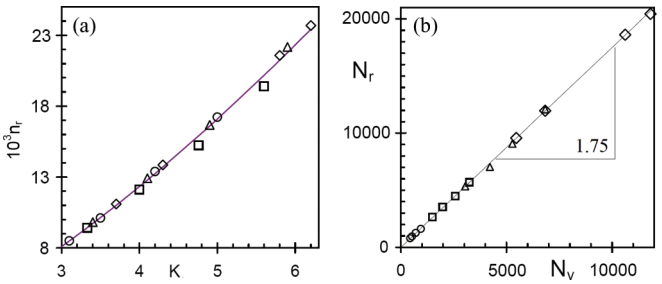

FIG. 3. Graphs of (a) normalized number $n_r = N_r(h/L)^{\phi}$ versus the confinement ratio K; and (b) N_r versus N_v for crumpling network impressions on sheets of size $L = 5$ (circles), 10 (squares), 15 (triangles), and 20 cm (rhombs). Fitting curves: $n_r = 0.001625K^{1.4622}$ ($R^2 = 0.99$) and $N_r = 1.75N_v$ ($R^2 = 0.99$).

Furthermore, with the help of the BENOIT1.3 software [54] we found that the number of square boxes of size Δ needed for the network covering obeys the scaling behavior,

$$N_{\text{box}} \propto \left(\frac{L}{\Delta}\right)^{D^{(2)}_N}, \tag{13}$$

within the interval of length scale $\Delta_c \leqslant \Delta \leqslant L/4$ (see Fig. 4) with the universal (independent of L and K) fractal (box-counting) dimension

$$D^{(2)}_N = 1.83 \pm 0.02, \tag{14}$$

while the lower cutoff of self-similarity ($\Delta_c \gg h$) is found to decrease as K increases (see bottom inset in Fig. 4). Although the intervals $\Delta_c \leqslant \Delta \leqslant L/4$ are of the order of one decade, we found that the data for all 16 crumpling networks of different sizes can be well collapsed to the single line on the log-log plot of normalized number of boxes $N^* = N_{\text{box}}(\Delta)/N_{\text{box}}(\Delta_C)$ versus Δ/Δ_C with the slope given by Eq. (14) (see top inset in Fig. 4). Once more, the relevance of the power-law fit is confirmed by the χ^2 test for goodness of fit.

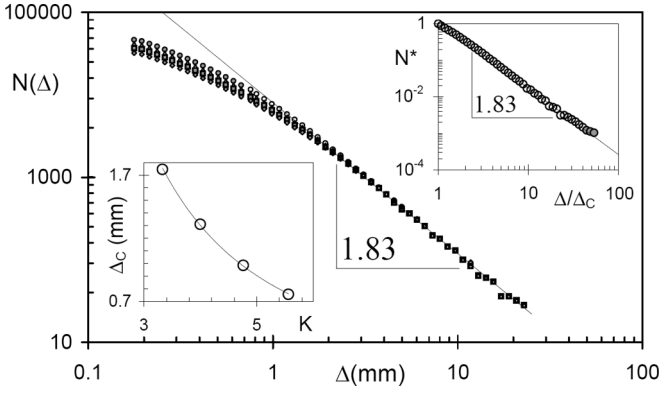

FIG. 4. Log-log plots of numbers of boxes covering the crumpling network images shown in Fig. 2 versus box size Δ in mm for K =5.6 (circles), 4.76 (triangles), 4 (squares), 3.33 (rhombs); full symbols corresponding to $\Delta < \Delta_C$ are excluded from fitting. Insets show the plots of (bottom) Δ_C (in mm) versus K; (top) normalized number of boxes $N^* = N(\Delta)/N(\Delta_C)$ versus Δ/Δ_C averaged over 16 crumpling network impressions.

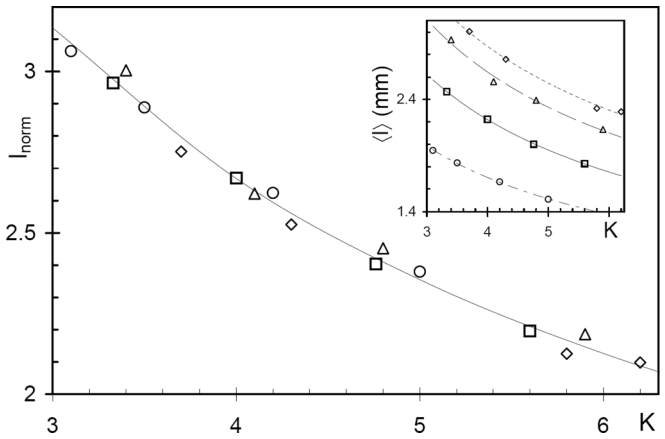

FIG. 5. Graph of normalized dimensionless mean ridge length $l_{\rm norm} = (\langle l\rangle/h)(L/h)^{-\theta}$ versus K; curve: data fitting $l_{\rm norm} = 5.8K^{-\alpha}$. Inset shows the graphs of in mm versus dimensionless compaction ratio K) for sheets of size L = 5 (circles), 10 (squares), 15 (triangles), and 20 cm (rhombs); curves: data fittings with Eq. (15).

From Eqs. (10) and (13) it follows that the mean ridge length should scale with the sheet size and compression ratio as

$$\langle l\rangle \propto L\left(\frac{L}{h}\right)^{-\theta} K^{-\alpha}, \tag{15}$$

instead of the first scaling relation in Eq. (2). We found that our experimental data (see Fig. 5) are consistent with Eq. (15) with the scaling exponents

$$\theta = \phi/D_N^{(2)} = 0.33 \pm 0.1 \quad \text{and} \quad \alpha = \gamma/D_N^{(2)} = 0.8 \pm 0.1, \tag{16}$$

which are calculated with values of ϕ, γ, and $D_N^{(2)}$ given in Eqs. (11) and (14), respectively.

Furthermore, we found that the scaling behavior (8) is robust over more than 500 realizations. Accordingly, we found that the fractal dimension of the minimum path on the crumpling network

$$d_{\rm min}^{(2)} = 1.15 \pm 0.06 \tag{17}$$

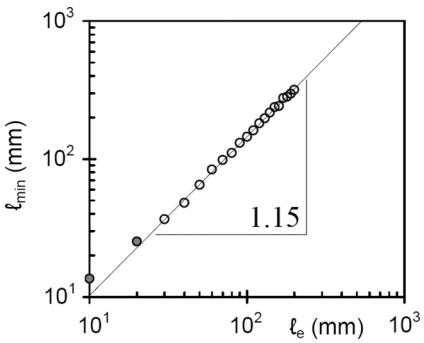

FIG. 6. Log-log plot of chemical distance $\ell_{\rm min}$ versus Euclidean distance ℓ_e between two randomly chosen points of crumpling network impression averaged over 16 networks; fitting curve $\ell_{\rm min} = 0.72\ell_e^{1.15}$, $R^2 = 0.99$ (full circles are excluded from fitting).

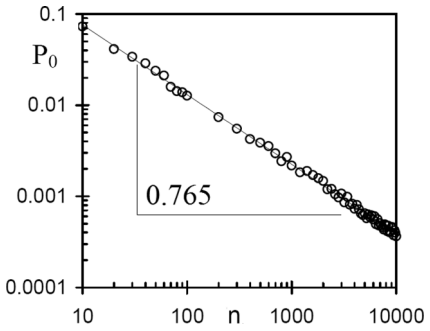

FIG. 7. Log-log plot of probability $P_0(n)$ to find (still or again) the random walker at step n at the randomly chosen starting vertex versus n. Data are averaged over 16 networks with 10^5 RW trajectories in each.

is independent of L and K (see Fig. 6) and so the chemical dimension of crumpling network impression

$$d_\ell^N = D_N^{(2)}/d_{\rm min}^{(2)} = 1.6 \pm 0.1 \tag{18}$$

is also independent of the sheet size and compression ratio.

Finally, the log-log plot of $P_0(n)$ in Fig. 7 provides the spectral dimension

$$d_s^N = 1.53 \pm 0.06, \tag{19}$$

which is independent of the sheet size and confinement ratio. It should be emphasized that data presented in Fig. 7 were obtained by averaging over 10^5 RW trajectories with about of 10^4 steps each, which were started from randomly chosen vertices of 16 analyzed crumpling networks. Accordingly, using the Alexander-Orbach law [55], we found that the random walk dimension of the crumpling network impression is

$$D_W^{(2)} = 2D_N^{(2)}/d_s^N = 2.39 \pm 0.12, \tag{20}$$

whereas the RW in the chemical space of the crumpling network is characterized by the random walk dimension $d_W^N = 2d_\ell^N/d_s^N = 2.09 \pm 0.20 > d_\ell^N$.

III. DISCUSSION

The knowledge of fractal dimensionalities ($D_N^{(2)}$, d_ℓ^N, and d_s^N) and scaling exponents (γ and ϕ) is of crucial importance for understanding the crumpling phenomena and the properties of randomly folded thin materials. In fact, these parameters govern the geometry, mechanics, and dynamics of hand crushed paper. Moreover, as will be argued below, the fractal dimensionalities of the crumpling network in the flat state are expected to be universal, whereas the value scaling exponents (γ, ϕ) and fractal dimensionalities of the crumpled network in the folded configurations are dependent on the crumpling geometry (hydrostatic, radial, uniaxial, and hand confinement) and rheological properties of the sheet.

A. Scaling properties of crumpling network impressions

Regarding data reported in the previous section, it is noteworthy to note that the fractal dimension (14) of crumpling network impressions with mean node degree (12) is less than the chemical dimension of the Sierpinski carpet with $\langle k\rangle = 4$

($d_\ell^{SC} = \ln 8/\ln 3 = D_{SC}$) and close to the fractal dimension of the Sierpinski gasket with $\langle k\rangle = 3$ ($d_\ell^{SG} = \ln 3/\ln 2 = D_{SG}$), whereas $d_{\min}^{(2)} > d_{\min}^{SC} = d_{\min}^{SG} = 1$ due to the tortuosity of the shortest paths in the crumpling network impression and so $D_N^{(2)} > D^{SG}$, but $D_N^{(2)} < D^{SC}$. Besides, it is interesting to note that the value (17) is numerically close to the minimum path dimension on the backbone of the percolation cluster on a two-dimensional network (see Ref. [56]).

On the other hand, we noted that the fractal dimension of the crumpling network impression (14) at least numerically coincides with the fractal dimension of clusters formed in the two-dimensional fuse network model with high disorder $D_{cl} = 1.86 \pm 0.01$ (see [61]). Although this coincidence can be accidental, it also may indicate that both processes belong to the same universality class. In this context, we also noted that although the fuse network model is used in Ref. [61] to study the fracturing of highly disordered materials, a remarkable resemblance between networks of localized folds in the thin films and fractures in drying pastes was pointed out in Ref. [62]. Moreover, the authors of Ref. [63] have stated that close to the stiffness divergence the buckling of the sheet is hindered by sheet thickness, such that its elastic behavior becomes similar to that of dry granular media. So, the coincidence of fractal dimensions D_{cl} and D_l can have a fundamental nature. If so, the two-dimensional fuse network model with disorder introduced by random boundary conditions can be used to simulate the crumpling of two-dimensional matter, e.g., the nanosheets crumpled by capillary forces in aqueous suspension [64] and geological formations (see Ref. [16]). However, for strict demonstration that forced crushing of self-avoiding elastic sheets belongs to the universality class of a two-dimensional fuse network model with high disorder, it is imperative to establish that the chemical and spectral dimensions are also equal for both systems.

Here we determine the spectral dimension of crumpling networks formed in randomly crumpled two-dimensional matter. So, it is pertinent to note that the experimental value (19) is within the expected range (see Ref. [55]) of

$$\frac{2d_\ell^N}{d_\ell^N + 1} = 1.24 \pm 0.03 \leqslant d_s^N = 1.53 \pm 0.05 \leqslant d_\ell^N, \qquad (21)$$

where the chemical dimension is provided by Eq. (18). Notice also that d_s^N is larger than the spectral dimension of percolation clusters and their backbones in two and three dimensions (see Ref. [65]), but it is less than the spectral dimensions of folded proteins ($1.6 \leqslant d_s^{\text{protein}} \leqslant 1.95$) reported in Ref. [9].

B. Fractal properties of crumpling network in the folded configuration

Mathematically, folding of self-avoiding two-dimensional sheets can be viewed as a continuum of isometric embeddings of a two-dimensional manifold in three-dimensional space [14,19]. The chemical dimension of a folded sheet is, per definition, equal to the chemical dimension of a flat sheet, that is, $d_\ell^{\text{ball}} = 2$. Therefore, the dimension of shortest path in a ball folded from a thin sheet is

$$d_{\min}^{\text{ball}} = D_l/d_\ell^{\text{ball}} = D_l/2, \qquad (22)$$

and so, in the case of hand crushed elastoplastic papers, which after complete elastic strain relaxation are characterized by the universal $D_l \approx 8/3$, the minimum path dimension $d_{\min}^{\text{ball}} \approx 4/3$ is also universal. However, in the case of randomly crumpled elastic (e.g., rubber) and predominantly plastic (e.g., aluminum foil) sheets the local fractal dimension defined by Eq. (7) and so $d_{\min}^{\text{ball}}$ defined by Eq. (22) are dependent on K and the mechanical properties of the sheet (see Ref. [30]). Moreover, it is easy to understand that the fractal dimension of RW in the chemical space of a folded ball is equal to the random walk dimension on the flat sheet ($d_W^{\text{ball}} = 2$), unless the jumps in self-contacting zones are permitted. Therefore, the random walk dimension of a folded sheet is $D_W^{\text{ball}} = d_{\min}^{\text{ball}} d_W^{\text{ball}} = D_l$. However, dynamic properties of a randomly crushed sheet are governed by the spectral dimension of the crumpling network.

In this context, it is a straightforward matter to demonstrate that the spectral dimension of a crumpling network in the folded configuration of a self-avoiding sheet is the same as found for the crumpling network impression. In fact, per definitions, the chemical dimension and the dimension of random walk in the chemical space of a crumpled network in the folded configuration are the same as in the unfolded (flat) state. That is,

$$\begin{aligned} d_\ell^N &= D_N^{(3)}/d_{\min}^{(3)} = D_N^{(2)}/d_{\min}^{(2)} \quad \text{and} \\ d_W^N &= D_W^{(3)}/d_{\min}^{(3)} = D_W^{(2)}/d_{\min}^{(2)}, \end{aligned} \qquad (23)$$

where $d_{\min}^{(3)}$ is the fractal dimension of the minimum path on the crumpled network in the folded configuration. Therefore, the Alexander-Orbach law (see Ref. [55]) implies that the spectral dimension of a folded crumpling network,

$$d_s^N = \frac{2D_N^{(3)}}{D_W^{(3)}} = \frac{2d_\ell^N}{d_W^N} = \frac{2D_N^{(2)}}{D_W^{(2)}}, \qquad (24)$$

has the value given by Eq. (19). Notice that the last equality in Eq. (24) does not hold in the case of crumpling networks formed in randomly folded phantom sheets, because due to the network intersection the second equality in Eq. (22) fails.

To determine the fractal dimension $D_N^{(3)}$ and the fractal dimension of the shortest path $d_{\min}^{(3)}$ for crumpling networks in the folded configuration, we noted that the folded network can be covered ether by two-dimensional boxes of size Δ, or by three-dimensional boxes of size δ such that $N_{\text{box}} \propto \delta^{D_N^{(3)}}$. The mass conservation implies that $\delta^{D_l} \propto \Delta^2$ and so

$$N_{\text{box}} \propto \delta^{D_l D_N^{(2)}/2} \propto \delta^{D_N^{(3)}}, \qquad (25)$$

such that

$$D_N^{(3)} = \frac{D_l D_N^{(2)}}{2} = d_{\min}^{\text{ball}} D_N^{(2)}. \qquad (26)$$

Accordingly,

$$d_{\min}^{(3)} = \left(D_N^{(3)}/D_N^{(2)}\right) d_{\min}^{(2)} = d_{\min}^{\text{ball}} d_{\min}^{(2)}. \qquad (27)$$

Consequently, the random walk dimension of the folded crumpling network is

$$D_W^N = 2D_N^{(3)}/d_s^N = d_W^N d_{\min}^{(3)}. \qquad (28)$$

For convenience, the fractal properties of crumpling networks in the flat and folded configurations are summarized in Table I

TABLE I. Fractal properties of hand folded paper sheets and crumpling networks.

	Balls folded from paper sheet	Crumpling network	
		On unfolded flat sheet	In sheet folded in ball
Chemical dimension	2	1.6 ± 0.1 (≈5/3)	
Global mass dimension (of a set of balls)	Dependent on the folding conditions	Not defined	
Local mass dimension	2.64 ± 0.06 [12,14] (≈8/3)	1.83 ± 0.02 (Fig. 4); =11/6 [Eq. (42)]	2.43 ± 0.05 (=22/9)
Dimension of shortest path	1.32 ± 0.03 [Eq. (22)] (≈4/3)	1.15 ± 0.06 (Fig. 6) (≈11/10)	1.53 ± 0.16 [Eq. (27)]
Dimension of RW in the chemical space	2	2.1 ± 0.2 (≈20/9)	
RW dimension	$D_W = D_l$	2.39 ± 0.12	3.2 ± 0.2
Spectral dimension	2	1.53 ± 0.06 (Fig. 7) (≈3/2)	

together with the fractal dimensionalities of hand folded paper balls. The knowledge of fractal dimensionalities is important to understand crumpling phenomena and to model mechanical and dynamical behavior of randomly folded materials. In this regard, it should be emphasized that in contrast to fractal dimensionalities d_ℓ^N, d_s^N, d_W^N, $D_N^{(2)}$, and $d_{\min}^{(2)}$ which are expected to be universal for randomly folded matter, the fractal dimensionalities of a crumpling network in the folded configuration ($D_N^{(3)}$, $d_{\min}^{(3)}$, and $D_W^{(3)}$) are material dependent, because the folding arrangement of paper is characterized by the universal dimension D_l only after complete relaxation of elastic strains [11,12], whereas D_l of randomly folded aluminum foil is dependent on the confinement ratio [30]. Nonetheless, following the arguments leading to Eq. (26) it is a straightforward matter to understand that the fractal dimension of clusters formed in the folded two-dimensional self-avoiding fuse network will be equal to the fractal dimension of a crumpling network in the folded configuration with the same D_l even when D_l is not universal.

C. Folding mechanics

The total elastic energy stored in a single crumpling ridge of length l is $E_r \propto h^3(l/h)^{1/3}$, while the ridge width is $w \propto h^{1/3}l^{2/3}$ [44]. However, the interactions between crumpling creases in a randomly folded sheet can alter the power-law scaling, such that more generally, $E_r \propto h^3(l/h)^\beta$ [33]. Furthermore, from the empirical relations (10) and (15) it follows that the total elastic energy stored in the crumpling network should obey the following scaling relation:

$$E_N \propto h^3\left(\frac{L}{h}\right)^{\phi+\beta(1-\theta)} K^{\gamma-\alpha\beta} \propto h^\varphi L^\zeta R^{-\mu+1}, \tag{29}$$

which differs from the relation (3) suggested in Ref. [33]. Consequently, the force-scaling exponent in Eq. (4) can be expressed as

$$\mu = \gamma - \alpha\beta + 1 = \gamma\left(1 - \beta/D_N^{(2)}\right) + 1, \tag{30}$$

while

$$\begin{aligned} \varphi &= 3 - \beta\left(1 - \phi/D_N^{(2)}\right) - \phi, \quad \text{and} \\ \zeta &= \phi + \beta\left(1 - \phi/D_N^{(2)}\right) + \gamma\left(1 - \beta/D_N^{(2)}\right), \end{aligned} \tag{31}$$

and so, the set of balls folded from "ideally elastic" self-avoiding sheets of different sizes under the same confinement force will obey the scaling relation (1) with the fractal dimension

$$D = 2\frac{D_N^{(2)}(1+\gamma) - \gamma\beta}{D_N^{(2)}(\beta+\phi+\gamma) - \beta(\gamma+\phi)} \tag{32}$$

instead of Eq. (6). Notice that in the case of phantom sheets crumpled under hydrostatic compression it is well established theoretically and by numerical simulations that $D = \mu = 8/3$ [23], while $\beta = 1/3$, $\phi = 0$, $\gamma = 2$, $\alpha = 1$ [44], and so $D_N^{(2)} = 2$. Hence, relationships (29)–(31) are held. However, $D_N^{(3)}$ cannot be defined, because relation (22) is not valid for the phantom sheets with intersection. Nonetheless, it is reasonable to expect that crumpling networks in phantom sheets under radial and uniaxial confinements are characterized by the same scaling exponents $\beta = 1/3$, $\phi = 0$, and $D_N^{(2)} = 2$. Consequently, using the values of μ obtained in Ref. [23] for phantom sheets under radial and uniaxial confinements (see Table II), from Eqs. (15), (29), and (30) we found that the mean ridge length in a phantom sheet crumpled under radial confinement will scale as $\langle l\rangle \propto L^{1/3}R^{2/3} \propto V_2^{1/3}$, whereas under uniaxial confinement $\langle l\rangle \propto L^{2/3}R^{1/3} \propto V_1^{1/3}$, such that generally,

$$\langle l\rangle \propto V_n^{1/3}, \tag{33}$$

where

$$V_n \propto L^3K^{-n} \tag{34}$$

is the volume occupied by the crumpled sheet, while n is the degree of compaction ($n = 1$ in the case of uniaxial, $n = 2$ radial, and $n = 3$ hydrostatic confinement, respectively). Accordingly, in the case of phantom sheets $N_r \propto K^{-2n/3}$ and so

$$\gamma = 2n/3 \quad \text{and} \quad \mu = 1 + 5\gamma/6 = 1 + 5n/9, \tag{35}$$

in accordance with results of numerical simulations [23] (see Table II).

In the case of self-avoiding elastic sheets, under the assumption that $\beta = 1/3$ (as is suggested by numerical simulations [33]) and universal $D_N^{(2)}$ (as it is expected if sheet crumpling belongs to the universality class of a two-dimensional fuse network model with high disorder) from Eqs. (29), (30),

TABLE II. Force-confinement exponent μ and scaling exponents γ and α for crumpling networks formed in two-dimensional sheets with different crumpling geometries.

Confinement	Material [Reference]	μ	γ	ϕ
Hydrostatic	Phantom elastic sheet [23]	$8/3$[a]; 2.66[b]	2[a]; 2[b]; 2[c]	0[a]
Radial	Phantom elastic sheet [23]	$19/9$[a]; 2.1[b]	$4/3$[c]	0[a]
Uniaxial	Phantom elastic sheet [23]	$14/9$[a]; 1.55[b]	$2/3$[c]	0[a]
Hydrostatic compression	Self-avoiding elastic sheet [23]	4[b]	$\approx$4[b]; 3.66[c]	0.18[d]
	Self-avoiding elasto-plastic sheet [33]	3.8 ± 0.1[b]	3.3[b]; 3.4[c]	
	Aluminum foil [29]	5.1[e]	5[c]	0.1[d]
	Aluminum foil [27]	4.76[e]	4.6[c]	0.06[d]
Radial crumpling	Self-avoiding elastic sheet [23]	3[b]	2.4[c]	–
Crushing in hands	*Biblia* paper (this work)	2.2 ± 0.1[c]	1.46 ± 0.05[e]	0.6 ± 0.1[e]
Uniaxial crumpling	Self-avoiding elastic sheet [23]	2[b]	1.22[c]	–
	Tethered membrane [63]	1.85[b]	1[c]	–
	Mylar [47]	1.89[e]	1.1[c]	–
	Paper [43]	1.3[e]	0.4[c]	–

[a]Theoretical values.
[b]Results of numerical simulations.
[c]Calculated with Eq. (30) with $\beta = 1/3$, while $D_N^{(2)} = 11/6$ for self-avoiding and $D_N^{(2)} = 2$ for phantom sheets.
[d]Calculated with Eq. (32) with $\beta = 1/3$, while $D_N^{(2)} = 11/6$ for self-avoiding and $D_N^{(2)} = 2$ for phantom sheets.
[e]Experimental values.

and (34) it follows that

$$\mu = 1 + 0.82\gamma, \tag{36}$$

where $\gamma(n)$ is an increasing function of the degree of compaction. In numerical simulations of self-avoiding elastic sheets under hydrostatic compression it was found that $\mu = 4$ [23]. Hence, according to Eq. (36) $\gamma = 3.66$, that is consistent with $\gamma \approx 4$ reported in Ref. [23]. Consequently, in the case of crumpling of ideally elastic self-avoiding sheets,

$$\gamma = \left(1 - \frac{\beta}{D_N^{(2)}}\right)^{-1} n = 1.22n \quad \text{and} \quad \alpha = \frac{n}{D_N^{(2)} - \beta}, \tag{37}$$

such that

$$\mu = 1 + n, \tag{38}$$

in accordance with the results of numerical simulations [23] (see Table II). It is pertinent that relation (38) was obtained in Ref. [23] from quite different arguments. In this context, the main point of our framework is that the mean ridge length in a self-avoiding elastic sheet under increasing confinement behaves as

$$\langle l \rangle \propto a^{-1} V_n^{2/3}, \tag{39}$$

in contrast to Eq. (33) for a phantom elastic sheet. Hence, self-avoiding interactions in a randomly crushed sheet introduce characteristic length scale

$$a = L(L/h)^{\theta} \tag{40}$$

governing the geometry and mechanics of crumpling phenomena. Furthermore, it should be emphasized that Eqs. (28) and (39) are consistent if and only if

$$D_N^{(2)} - \beta = 3/2, \tag{41}$$

and so

$$D_N^{(2)} = 11/6, \tag{42}$$

if $\beta = 1/3$. The fact that the fractal dimension of crumpling networks in ideally elastic sheets (42) is the same as found experimentally for elastoplastic paper (14) supports the statement of its universality, as well as the universality of $\beta = 1/3$.

To determine scaling exponents θ and $\phi = \theta D_N^{(2)}$ we noted that a set of self-avoiding elastic sheets folded under the same hydrostatic force obeys the scaling relation (1) with the fractal dimension (32). In numerical simulations it was found that $D = 2.3$ [23] and so $\phi = 0.18$ and $\theta = 0.1$. It is easy to understand that a set of sheets crumpled by the same radial or axial force will obey the scaling relation (1) with different D and so $\theta(n)$ and $\phi(n) = \theta D_N^{(2)}$ are dependent on the crumpling geometry characterized by the degree of compaction (n). Furthermore, the plastic deformations can lead to deviation from scaling behavior (39), such that the relationships (37) and (38) do not hold anymore. Nonetheless, the force scaling exponent μ is related to γ as is defined by Eq. (36) as long as the relationship (41) holds. Accordingly, in Table II we present the values of γ for different elastoplastic materials crumpled under different confinement conditions which were calculated with experimental values of μ reported in the literature. On the other hand, using the experimental value of γ for hand crumpled paper (11) we calculated the force exponent μ for the case of hand crushing (see Table II).

As follows from data reported in Table II, hand crushing resembles the radial crumpling ($n = 2$) rather than hydrostatic confinement ($n = 3$). This is consistent with the concept of fractional geometry of compaction, introduced in Ref. [43]. Moreover, our approach permits us to explicitly express the fractal dimension of compaction D_c in terms of network parameters. Namely, in the case of self-avoiding sheets, it is expected that the mean length of crumpling ridges obeys the scaling relation (33), but, generally,

$$V_n \propto L^3 K^{-D_c}, \tag{43}$$

and so

$$\gamma = \frac{2D_c D_N^{(2)}}{3}, \quad \text{while} \quad \mu = 1 + \frac{2}{3}D_c\left(D_N^{(2)} - \beta\right), \quad (44)$$

where $0 < D_c \leqslant 1$ in the case of axial confinement, $1 < D_c \leqslant 2$ in the case of biaxial or radial crushing, and $2 < D_c \leqslant 3$ in the case of three-dimensional compression. Specifically, the hand crushing is characterized by $D_c = 1.2$, whereas experiments reported in Ref. [43] are characterized by $D_c = 0.3$. It is pertinent to note that the values $1 \leqslant \mu \leqslant 2$ explain relative low resistance to axial compaction ($0 < D_c \leqslant 1$), whereas the resistance of a folded paper ball to hydrostatic compression ($2 < D_c \leqslant 3$) is enormously high ($\mu > 3$). Moreover, in the case of aluminum foil crumpled under hydrostatic pressure, the values of $\mu > 4$ [27,29] indicate that scaling relations (43) and (44) fail due to plastic deformations, whereas Eqs. (29)–(32) remain valid (see Table II). Likewise, it is important to point out that under the increasing hydrostatic confinement the folding configurations exhibit a phase transition associated with the spontaneous symmetry breaking [30] and accompanied by the change of the force-confinement ratio relation [29].

Since our approach to crumpling mechanics is generic, it provides a general framework to model the crushing phenomena in any scale from crumpled graphene structures to geological formations. Furthermore, the knowledge of fractal properties of a crumpling network (see Tables I and II) permits us to map mechanics problems for the fractal ball into the corresponding problems for fractal continua $\frac{d_s^N}{d_l^N}\Phi_D^3$ (see Ref. [66]).

IV. CONCLUSIONS

Summarizing, we found that under an increasing confinement the network degree distribution remains invariant with the universal mean $\langle k \rangle = 3.5 \pm 0.1$, whereas the number (10) and mean length (15) of crumpling ridges are the power-law functions of sheet thickness, linear size, and confinement ratio. Furthermore, we determined the chemical (18) and spectral (19) dimensions of crumpling networks formed in randomly folded two-dimensional matter. It is argued that the fractal dimensionalities of crumpling networks in the flat and folded configurations are universal, whereas the scaling exponents governed behavior of the mean ridge length and total number of ridges under the increasing confinement ratio are dependent on the crumpling geometry. The possible use of the two-dimensional fuse network model with high disorder to simulate the crumpling phenomena in different physical systems is discussed.

The knowledge of fractal properties of a crumpling network permits us to model mechanical and dynamic behavior of randomly crushed matter. In this way, we state that self-avoiding interactions introduce a characteristic length scale (40) of sheet crumpling. Accordingly, mechanics of sheet crushing is revised. Some useful scaling relations are derived. The effect of compaction geometry on crushing mechanics is revealed. These results provide a physically based framework to study the crumpling phenomena in quite different systems from graphene based nanosheets to geological formations.

ACKNOWLEDGMENTS

This work was supported by the PEMEX under the research SENER-CONACYT Grant No. 143927.

[1] J. Zhang, J. Xiao, X. Meng, C. Monroe, Y. Huang, and J.-M. Zuo, Phys. Rev. Lett. **104**, 166805 (2010); K. Kim, Z. Lee, B. D. Malone, K. T. Chan, B. Alemán, W. Regan, W. Gannett, M. F. Crommie, M. L. Cohen, and A. Zettl, Phys. Rev. B **83**, 245433 (2011); C. N. Lau, W. Bao, and J. Velasco, Jr., Mater. Today **15**, 238 (2012); N. B. Le and L. M. Woods, Phys. Rev. B **85**, 035403 (2012).

[2] J. Luo, H. D. Jang, T. Sun, L. Xiao, Z. He, A. P. Katsoulidis, M. G. Kanatzidis, J. Murray Gibson, and J. Huang, ACS Nano **5**, 8943 (2011); J. Agbenyega, Mater. Today **14**, 578 (2011).

[3] S. W. Cranford and M. J. Buehler, Phys. Rev B **84**, 205451 (2011).

[4] Y. Chen, F. Guo, A. Jachak, S.-P. Kim, D. Datta, J. Liu, I. Kulaots, C. Vaslet, H. D. Jang, J. Huang, A. Kane, V. B. Shenoy, and R. H. Hurt, Nano Lett. **12**, 1996 (2012); S. Mao, Z. Wen, H. Kim, G. Lu, P. Hurley, and J. Chen, ACS Nano **6**, 7505 (2012); C. D. Zangmeister, X. Ma, and M. R. Zachariah, Chem. Mater. **24**, 2554 (2012); J. Kim, L. J. Cote, and J. Huang, Acc. Chem. Res. **45**, 1356 (2012).

[5] X. Ma, M. R. Zachariah, and C. D. Zangmeister, Nano Lett. **12**, 486 (2012).

[6] W.-N. Wang, Y. Jiang, and P. Biswas, J. Phys. Chem. Lett. **12**, 3228 (2012).

[7] T. Haliloglu, I. Bahar, and Burak Erman, Phys. Rev. Lett. **79**, 3090 (1997); R. Bundschuh and T. Hwa, *ibid.* **83**, 1479 (1999); J. Xu, Z. Zhu, S. Luo, C. Wu, and S. Liu, *ibid.* **96**, 027802 (2006); V. S. Pande, *ibid.* **105**, 198101 (2010); E. Karzbrun, J. Shin, R. H. Bar-Ziv, and V. Noireaux, *ibid.* **106**, 048104 (2011); N. Stoop, J. Najafi, F. K. Wittel, M. Habibi, and H. J. Herrmann, *ibid.* **106**, 214102 (2011); A. V. Finkelstein and O.V. Galzitskaya, Phys. Life Rev. **1**, 23 (2004); S. Kumara and M. S. Li, Phys. Rep. **486**, 1 (2010).

[8] R. Granek and J. Klafter, Phys. Rev. Lett. **95**, 098106 (2005); S. Reuveni, R. Granek, and J. Klafter, *ibid.* **100**, 208101 (2008); M. A. Moret, M. C. Santana, G. F. Zebende, and P. G. Pascutti, Phys. Rev. E **80**, 041908 (2009); G. Lois, J. Blawzdziewicz, and C. S. O'Hern, *ibid.* **81**, 051907 (2010); R. Granek, *ibid.* **83**, 020902(R) (2011); I. V. Kalgin and S. F. Chekmarev, *ibid.* **83**, 011920 (2011); S. Reuveni, J. Klafter, and R. Granek, *ibid.* **85**, 011906 (2012).

[9] E. Tejera, A. Machado, I. Rebelo, and J. Nieto-Villar, Physica A **388**, 4600 (2009).

[10] M. A. F. Gomes, J. Phys. A **20**, L283 (1987); M. A. F. Gomes, G. L. Vasconcelos, and C. C. Nascimento, J. Phys. A: Math. Gen. **20**, L1167 (1987); M. A. F. Gomes, T. I. Jyh, and T. I. Ren, *ibid.* **23**, L1281 (1990); J. B. C. Garcia, M. A. F. Gomes, T. I. Jyh, and T. I. Ren, *ibid.* **25**, L353 (1992);

E. M. Kramer and A. E. Lobkovsky, Phys. Rev. E **53**, 1465 (1996); P. A. Houle and J. P. Sethna, *ibid.* **54**, 278 (1996); M. A. F. Gomes and V. M. Oliveira, Philos. Mag. Lett. **78**, 325 (1998); R. Cassia-Moura and M. A. F. Gomes, J. Theor. Biol. **238**, 331 (2006).

[11] A. S. Balankin, O. Susarrey, R. Cortes, D. Samayoa, J. Martínez, and M. A. Mendoza, Phys. Rev. E **74**, 061602 (2006).

[12] A. S. Balankin, R. Cortes, and D. Samayoa, Phys. Rev. E **76**, 032101 (2007).

[13] A. S. Balankin, D. Samayoa, E. Pineda, R. Cortes, A. Horta, and M. A. Martínez Cruz, Phys. Rev. B **77**, 125421 (2008).

[14] A. S. Balankin, D. Samayoa, I. A. Miguel, J. Patiño, and M. A. Martínez Cruz, Phys. Rev. E **81**, 061126 (2010).

[15] A. S. Balankin, O. Susarrey, F. Hernández, and J. Patiño, Phys. Rev. E **84**, 021118 (2011).

[16] N. Cardozo, R. W. Allmendinger, and J. K. Morgan, J. Struct. Geol. **27**, 1954 (2005); D. M. Hansen and J. Cartwright, *ibid.* **28**, 1520 (2006); Z. Ismat, *ibid.* **31**, 972 (2009); B. E. Hobbs, A. Ord, and K. Regenauer-Lieb, *ibid.* **33**, 758 (2011).

[17] M. J. Bowick and A. Travesset, Phys. Rep. **344**, 255 (2001).

[18] T. A. Witten, Rev. Mod. Phys. **79**, 643 (2007).

[19] A. S. Balankin, D. Morales, E. Pineda, A. Horta, M. A. Martínez Cruz, and D. Samayoa, Physica A **388**, 1780 (2009).

[20] R. F. Albuquerque and M. A. F. Gomes, Physica A **310**, 377 (2002).

[21] L. Bevilacqua, Appl. Math. Model. **28**, 547 (2004).

[22] D. L. Blair and A. Kudrolli, Phys. Rev. Lett. **94**, 166107 (2005).

[23] G. A. Vliegenthart and G. Gompper, Nat. Mater. **5**, 216 (2006).

[24] E. Sultan and A. Boudaoud, Phys. Rev. Lett. **96**, 136103 (2006).

[25] M. A. F. Gomes, C. C. Donato, S. L. Campello, R. E. de Souza, and R. Cassia-Moura, J. Phys. D: Appl. Phys. **40**, 3665 (2007).

[26] Ch. A. Andresen, A. Hansen, and J. Schmittbuhl, Phys. Rev. E **76**, 026108 (2007).

[27] A. S. Balankin, I. Campos, O. A. Martínez, and O. Susarrey, Phys. Rev. E **75**, 051117 (2007).

[28] T. Tallinen, J. A. Aström, and J. Timonen, Phys. Rev. Lett. **101**, 106101 (2008); Comput. Phys. Commun. **180**, 512 (2009).

[29] Y. C. Lin, Y. L. Wang, Y. Liu, and T. M. Hong, Phys. Rev. Lett. **101**, 125504 (2008); W. Bai, Y.-C. Lin, T.-K. Hou, and T.-M. Hong, Phys. Rev. E **82**, 066112 (2010).

[30] Y.-C. Lin, J.-M. Sun, J.-H. Hsiao, Y. Hwu, C. L. Wang, and T.-M. Hong, Phys. Rev. Lett. **103**, 263902 (2009); Y.-C. Lin, J.-M. Sun, H. W. Yang, Y. Hwu, C. L. Wang, and T.-M. Hong, Phys. Rev. E **80**, 066114 (2009).

[31] A. S. Balankin and O. Susarrey, Phys. Rev. E **77**, 051124 (2008).

[32] I. Dierking and P. Archer, Phys. Rev. E **77**, 051608 (2008).

[33] T. Tallinen, J. A. Aström, and J. Timonen, Nat. Mater. **8**, 25 (2009).

[34] T. Tallinen, J. A. Aström, P. Kekalainen, and J. Timonen, Phys. Rev. Lett. **105**, 026103 (2010).

[35] H. Aharoni and E. Sharon, Nat. Mater. **9**, 993 (2010).

[36] D. Aristoff and C. Radin, Europhys. Lett. **91**, 56003 (2010).

[37] M. Adda-Bedia, A. Boudaoud, L. Boué, and S. Deboeuf, J. Stat. Mech. Theor. Exp. 11 (2010) P11027.

[38] A. Dominique Cambou and N. Menon, Proc. Natl. Acad. Sci. USA **108**, 14741 (2011).

[39] R. D. Schroll, E. Katifori, and B. Davidovitch, Phys. Rev. Lett. **106**, 074301 (2011).

[40] A. B. Thiria and M. Adda-Bedia, Phys. Rev. Lett. **107**, 025506 (2011); G. Seizilles, E. Bayart, M. Adda-Bedia, and A. Boudaoud, Phys. Rev. E **84**, 065602(R) (2011).

[41] A. S. Balankin, S. Matías, D. Samayoa, J. Patiño, B. Espinoza Elizarraraz, and C. L. Martínez-González, Phys. Rev. E **83**, 036310 (2011).

[42] H. Diamant and T. A. Witten, Phys. Rev. Lett. **107**, 164302 (2011); B. Roman and A. Pocheau, *ibid.* **108**, 074301 (2012); S. S. Datta, S.-H. Kim, J. Paulose, A. Abbaspourrad, D. R. Nelson, and D. A. Weitz, *ibid.* **109**, 134302 (2012); J. Hure, B. Roman, and J. Bico, *ibid.* **109**, 054302 (2012).

[43] S. Deboeuf, E. Katzav, A. Boudaoud, D. Bonn, and M. Adda-Bedia, Phys. Rev. Lett. **110**, 104301 (2013).

[44] A. Lobkovsky, S. Gentges, H. Li, D. Morse, and T. A. Witten, Science **270**, 1482 (1995); E. M. Kramer and T. A. Witten, Phys. Rev. Lett. **78**, 1303 (1997); G. Gompper, Nature **386**, 439 (1997); B. A. DiDonna, T. A. Witten, S. C. Venkataramani, and E. M. Kramer, Phys. Rev. E **65**, 016603 (2001).

[45] Finer analysis suggests the coexistence of two types of domains: (1) diffuse-stress regions characterized by a mechanical constraint associated with the dominance of a single component of the stress tensor, and (2) patches subjected to geometric, piecewise-inextensibility constraints (see Ref. [39]).

[46] B. A. DiDonna and T. A. Witten, Phys. Rev. Lett. **87**, 206105 (2001).

[47] K. Matan, R. B. Williams, T. A. Witten, and S. R. Nagel, Phys. Rev. Lett. **88**, 076101 (2002).

[48] In fact, two sets of balls folded under the fixed force and the fixed pressure are characterized by different D [19,30], whereas the ball structure is, obviously, independent of the way in which other balls were folded.

[49] M. Barthélémy, S. V. Buldyrev, S. Havlin, and H. E. Stanley, Phys. Rev. E **60**, R1123 (1999).

[50] K. Oleschko, G. Korvin, A. S. Balankin, R. V. Khachaturov, L. Flores, B. Figueroa, J. Urrutia, and F. Brambila, Phys. Rev. Lett. **89**, 188501 (2002); K. Oleschko, G. Korvin, B. Figueroa, M. A. Vuelvas, A. S. Balankin, L. Flores, and D. Carreón, Phys. Rev. E **67**, 041403 (2003).

[51] K. Oleschko, Soil Tillage Res. **52**, 247 (1999); K. Oleschko, G. Korvin, L. Flores, F. Brambila, C. Gaona, J. F. Parrot, G. Ronquillo, and S. Zamora, Geoderma **160**, 93 (2010).

[52] E. Feder, *Fractals* (Plenum, New York, 1988).

[53] A. S. Balankin and O. Susarrey, in *Proceedings of the IUTAM Symposium on Scaling in Solid Mechanics*, *Cardiff, UK, 25–29 June, 2007*, edited by F. M. Borodich (Springer, Berlin, 2009).

[54] BENOIT1.3, http://www.trusoft-international.com/benoit.html (2013); W. Seffens, Science **285**, 1228 (1999).

[55] S. Halvin and D. Ben-Avraham, Adv. Phys. **51**, 187 (2002).

[56] Z. Zhou, J. Yang, Y. Deng, and R. M. Zif, Phys. Rev. E **86**, 061101 (2012).

[57] U. Mosco, Phys. Rev. Lett. **79**, 4067 (1997).

[58] S. Weber, J. Klafter, and A. Blumen, Phys. Rev. E **82**, 051129 (2010).

[59] M. Werner and J.-U. Sommer, Phys. Rev. E **83**, 051802 (2011).

[60] K. Falconer, *Fractal Geometry: Mathematical Foundations and Applications* (Wiley, New York, 1990).

[61] A. A. Moreira, C. L. N. Oliveira, A. Hansen, N. A. M. Araújo, H. J. Herrmann, and J. S. Andrade, Phys. Rev. Lett. **109**, 255701 (2012).

[62] P. M. Reis, Nat. Mater. **10**, 907 (2011).

[63] J. A. Astrom, J. Timonen, and M. Karttunen, Phys. Rev. Lett. **93**, 244301 (2004).

[64] It is pertinent to note that in Refs. [5,6] it was pointed out that there is a quantitative similarity between scaling properties of nanosheets crumpled by capillary forces in aqueous suspension.

[65] M. Porto, A. Bunde, S. Havlin, and H. E. Roman, Phys. Rev. E **56**, 1667 (1997).

[66] A. S. Balankin and B. E. Elizarraraz, Phys. Rev. E **85**, 056314 (2012).